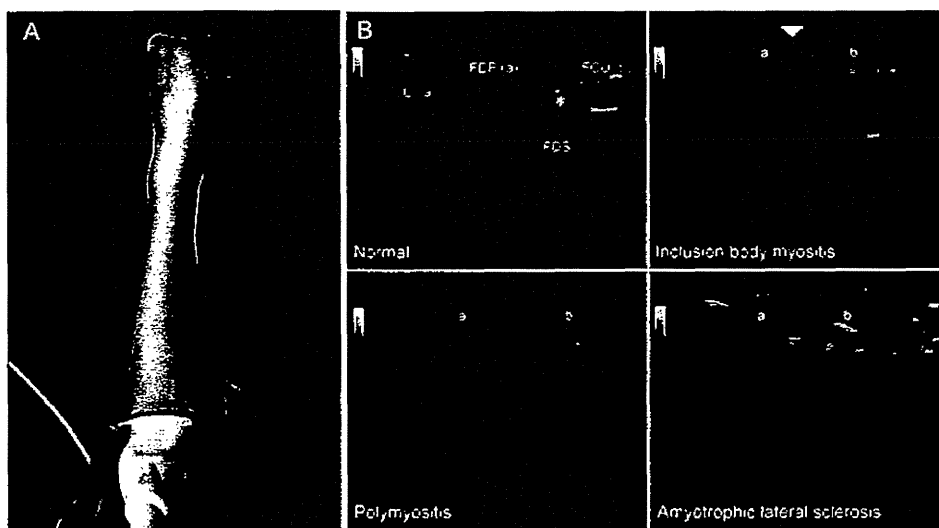


Noto et al., p14

**Table 2. Comparison of muscle cross-sectional area.**

	s-IBM (n = 6)	PM/DM (n = 6)	ALS (n = 6)
CSA of the FDP muscle (mm <sup>2</sup> ); mean (range)	80.5 (63.0-117.4)	165.9 (90.4-332.3)	106.3 (62.1-148.6)
CSA of the FCU muscle (mm <sup>2</sup> ); mean (range)	131.8 (100.9-149.5) †	110.3 (73.9-135.6)	86.3 (49.4-129.4)
FDP/FCU CSA ratio: mean	0.61 <sup>**†</sup>	1.47	1.28

**\*\*P < 0.01 vs. PM/DM. †P < 0.05 vs. ALS.** s-IBM, sporadic inclusion body myositis; PM/DM, polymyositis/dermatomyositis; ALS, amyotrophic lateral sclerosis; CSA, cross-sectional area; FDP, flexor digitorum profundus muscle; FCU, flexor carpi ulnaris muscle. FDP/FCU CSA ratio is defined as CSA of the FDP muscle divided by CSA of the FCU muscle.



136x75mm (300 x 300 DPI)

Accepted

## Three Spinocerebellar Ataxia Type 2 Siblings with Ataxia, Parkinsonism, and Motor Neuronopathy

Noriko Nishikawa<sup>1</sup>, Masahiro Nagai<sup>1</sup>, Tomoaki Tsujii<sup>1</sup>, Nachi Tanabe<sup>1</sup>,  
Hiroshi Takashima<sup>2</sup> and Masahiro Nomoto<sup>1</sup>

---

### Abstract

---

Spinocerebellar ataxia type 2 (SCA2) represents a family of dominant neurodegenerative disorders that results from CAG expansion repeat mutations. The phenotype consists of some common features, most notably progressive ataxia. We describe three siblings with SCA2, manifesting parkinsonism and ataxia in the first sibling, juvenile parkinsonism in the second and motor neuronopathy in the third. Genetic examination revealed expansion to 42, 43, and 42 CAG repeats. There was no relationship between the number of repeats and phenotype. The SCA2 gene should be studied in families with heterogeneous neurodegenerative disorders, including motor neuron disease.

**Key words:** SCA2, motor neuron disease, parkinsonism, ataxia, neurodegenerative disorders

(Intern Med 50: 1429-1432, 2011)

(DOI: 10.2169/internalmedicine.50.5262)

---

### Introduction

---

Autosomal dominant cerebellar ataxia type 2 is caused by CAG expansion in the coding region of the ataxin 2 gene on chromosome 12q23-24.1. The normal range of CAG repeats usually extends from 14 to 32 repeats, while it ranges from 35 to 50 or more in affected persons (1, 2). The clinical hallmark of spinocerebellar ataxia type 2 (SCA2) with juvenile onset is cerebellar gait and limb ataxia associated with slow eye movements and hyporeflexia. However, it has been shown recently that the phenotype of SCA2 is wider than previously believed. Patients may present with either a typical L-dopa-responsive parkinsonism or an atypical parkinsonism including signs of ataxia (3). There may be considerable intra- and interfamilial variation of clinical signs (4). We describe three siblings with SCA2 CAG expansion, one sibling presented with parkinsonism and ataxia, the second one with juvenile parkinsonism, and the third one with motor neuronopathy. We investigated the relationship between phenotype and genotype.

---

### Case Report

---

Three siblings were examined after obtaining permission to use their photographs and informed consent was obtained to take blood sampling for genetic study. Genomic DNAs were isolated from peripheral blood lymphocytes using the DNA Extractor WB kit (Wako, Japan). The regions containing the SCA2 CAG repeats were PCR-amplified using previously described gene-specific primers (5'-CCCTCACCATGTCGCTGAAGC-3' and 5'-3') (5). The number of the repeats in the fluorescent-labeled PCR products was estimated by Gene Scan analysis using an ABI PRISM 310 automated DNA sequencer (Applied Biosystems, Foster City CA USA), then, determined through the PCR products sequencing on an ABI PRISM 310 Genetic Analyzer using a Big Dye Terminator Cycle Sequencing Ready Reaction Kit (Applied Biosystems).

The proband (case 1: III-13) is a 59-year-old man. He had been well until 42 years of age, when he noticed gait difficulties. At 45 years, he was diagnosed with PD. His mother (II-8), sister (case 2: III-14), uncles (II-4,5) and aunts (II-2,7) of the mother's side had been treated under the diagno-

---

<sup>1</sup>Department of Neurology and Clinical Pharmacology, Ehime University Hospital, Japan and <sup>2</sup>Department of Neurology and Geriatric Medicine, Kagoshima University Graduate School of Medicine, Japan

Received for publication February 3, 2011; Accepted for publication March 23, 2011

Correspondence to Dr. Noriko Nishikawa, n-nishi@m.ehime-u.ac.jp

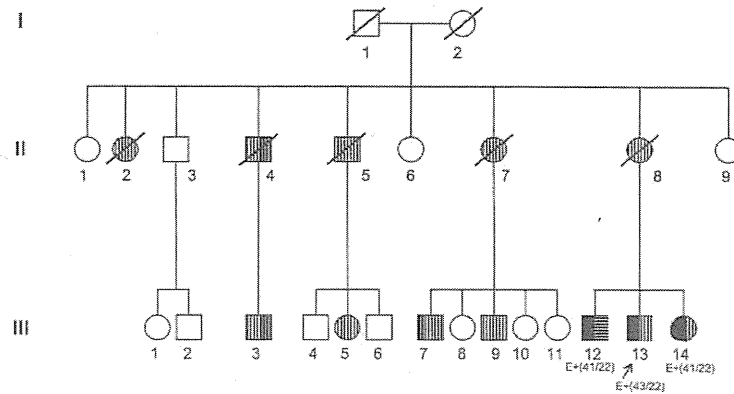


Figure 1. Pedigree of the three siblings. E+(CAG repeat numbers) indicate positive evaluation with the number of CAG repeats in the expanded and the normal alleles.

- Indicates SCA2
- ▨ Indicates parkinsonism
- ▧ Indicates motor neuronopathy

sis of Parkinson's disease. The family history suggested they were affected by hereditary parkinsonism with autosomal dominance (Fig. 1). He showed mild rigidity and bradykinesia. No limb or gait ataxia was noted. Levodopa/carbidopa was prescribed with marked benefit. The medication allowed him to perform activities of daily living. He kept his job as a local government employee until the age of 56. However, his symptoms progressed gradually. At the age of 57, he developed dysarthria and trunkal ataxia. Brain magnetic resonance imaging (MRI) study revealed brainstem and cerebellar atrophy (Fig. 2a).

Case 2 (III-14) is the younger 58-year-old female sibling of the proband (III-13). At age 39, she developed resting tremor and rigidity, and bradykinesia. She was diagnosed with juvenile PD. She responded to levodopa very well, keeping her job perfectly for 15 years as an office worker for an insurance company. She sometimes showed mild trunkal and leg dyskinesia during "ON" time with levodopa treatment. She did not show ataxia, abnormal eye movements, pyramidal signs, nor significant dysautonomia except for constipation. Brain MRI revealed no abnormalities. The ratio of myocardial  $^{123}\text{I}$ -metaiodobenzylguanidine (MIBG) scintigraphic uptake in regions of interest in the heart to that in the mediastinum (H/M ratio) was reduced (early 1.26, delay 1.09) (6). Her phenotype was indistinguishable from idiopathic PD.

Case 3 (III-12) is the elder 64-year-old male sibling of the proband (III-13). Marginal muscle weakness and atrophy in the upper limbs was noted at 14 years of age. The muscle weakness was slowly progressive. However, he could manage everything in his life as a business person up to the age of 60 years. He did not show signs or findings suggestive of poliomyelitis or exposure to toxic substances that cause muscle weakness. Neurological examination disclosed muscle atrophy in the neck, shoulder girdle, and limbs (Fig. 2b). He did not show ataxia, parkinsonism, or pyramidal signs. Brain MRI revealed no abnormalities. Electrophysiological

findings were consistent with a chronic neurogenic pattern. Nerve conduction study was normal with no evidence of conduction block. Compound muscle action potential was low, which was consistent with muscle atrophy.

The siblings had a normal allele with 22 repeats that sequencing showed glutamines were encoded by  $(\text{CAG})_8(\text{CAA})(\text{CAG})_8(\text{CAA})(\text{CAG})_8$ . The expanded allele of case 1 had 43 glutamine repeats encoded by  $(\text{CAG})_{34}(\text{CAA})(\text{CAG})_8$ . Case 2 and case 3 had 42 glutamine repeats encoded by  $(\text{CAG})_{33}(\text{CAA})(\text{CAG})_8$  (Fig. 3). The number of repeats was increased by two in case 1 compared to case 2 and case 3, and there were no differences between case 2 and case 3 in the genetic investigation.

## Discussion

This family had been noticed as being affected by hereditary PD with autosomal dominance. The proband case showed ataxia 12 years after the development of parkinsonism and was shown to have SCA2 mutation on gene analysis. Case 2 showed parkinsonism but did not develop ataxia until 19 years after PD onset, when she showed balance disturbance and CT scan confirmed mild cerebellar atrophy. MRI study did not show cerebellar atrophy. MIBG study revealed a decreased H/M ratio which is compatible with parkinsonism, while the other 2 cases (1 and 3) showed H/M ratio values of 2.1 and 1.9, respectively, which are normal. Case 3 developed bilateral muscular atrophy of the arms. Cases with SCA2 exhibiting muscular atrophy and cerebellar ataxia or rigidity have been previously reported (7, 8). Case 3 started to develop muscle weakness and atrophy of the arms at 14 years of age, which worsened very slowly. He was not affected by poliomyelitis, with his serum titer being lower than the detectable limit. Nerve conduction velocity was normal, but there was a suggestion of spinal cord motor neuron degeneration. The CAG repeat expansion in SCA2 gene was detected in case 3. Pathological

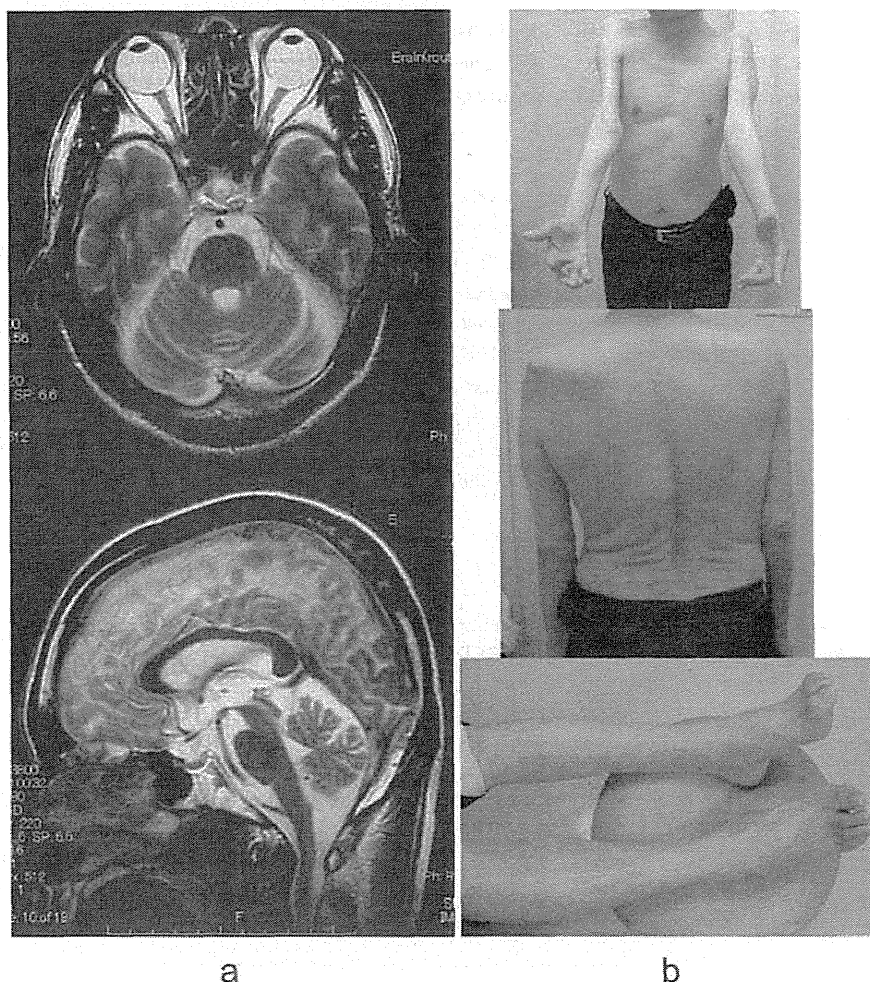


Figure 2. Brain MRI of case 1 (III-13) (a) and pictures of case 3 (III-12) (b).

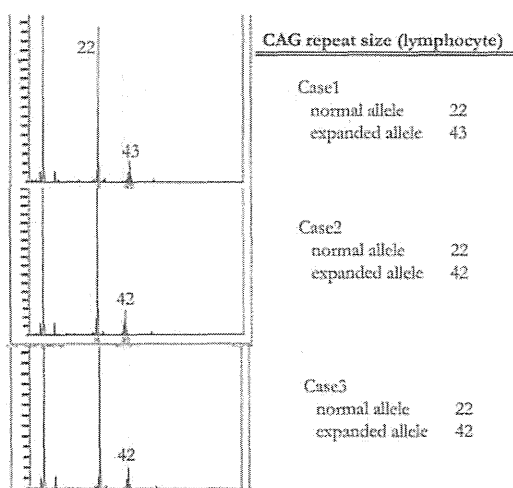


Figure 3. Fragment analysis of SCA2 gene in the three siblings.

study has previously revealed cases of SCA2 showing motor neuron degeneration (9). Case 3 (III-12) may be a phenotype of SCA2 and should be followed up for the possible development of ataxia or parkinsonism. Pathological study

will be recommended for the motor neuronopathy in the future.

Patients with parkinsonism-predominant SCA2 without ataxia have been recently described to respond dramatically to levodopa therapy. These cases are reported in Asians, but rarely in Caucasians. The present cases are compatible with these reports of PD (3, 4, 7). CAG repeats which were in the low expansion range and interrupted by CAA were associated with SCA2-related parkinsonism (10, 11). Another finding about SCA disease is the large variation of the phenotype. SCA2 has been classified by OPCA, and its phenotype seems to be related to the length of CAG repeats (12, 13). However there was no difference in the length on CAG repeats or the gene sequence in our siblings. Their phenotype varied and they were diagnosed as different disorders clinically. There may be other factors apart from the length or sequence of CAG repeats that determine SCA2 phenotype. CAG repeat size can be different between tissues such as cerebellum, pons, or spinal cord (14). Genotypic examination for SCA2 should be considered more widely because of the varied phenotype (15).

In conclusion, we have described three siblings with SCA 2, who developed juvenile parkinsonism, parkinsonism/

ataxia, and motor neuronopathy. Motor neuron symptoms and signs may be a manifestation in SCA2. The SCA2 gene should be studied in families with heterogeneous neurodegenerative disorders, including motor neuron disease.

The authors state that they have no Conflict of Interest (COI).

#### Acknowledgement

This work was supported by a grant-in-Aid from the Research Committee for CNS Degenerative Diseases, and Ataxic Diseases, the Ministry of Health, Labour and Welfare, Japan and SRF. Authors are thankful to Professor Masatoyo Nishizawa, Department of Neurology at Niigata University Hospital, for his consulting the patients and suggestions and support for this case report, and Ms Mika Kaneta for performing genetic analysis of the cases.

#### References

1. Gispert S, Twells R, Orozco G, et al. Chromosomal assignment of the second locus for autosomal dominant cerebellar ataxia (SCA2) to chromosome 12q23-24.1. *Nat Genet* 4: 295-299, 1993.
2. Pulst SM, Nechiporuk A, Nechiporuk T, et al. Moderate expansion of a normally biallelic trinucleotide repeat in spinocerebellar ataxia type 2. *Nat Genet* 14: 269-276, 1996.
3. Furtado S, Farrer M, Tsuboi Y, et al. SCA-2 presenting as parkinsonism in an Alberta family: clinical, genetic, and PET findings. *Neurology* 59: 1625-1627, 2002.
4. Lu CS, Wu Chou YH, Yen TC, Tsai CH, Chen RS, Chang HC. Dopa-responsive parkinsonism of spinocerebellar ataxia type 2. *Mov Disord* 17: 1046-1051, 2002.
5. Pulst SM, Nechiporuk A, Nechiporuk T, et al. Moderate expansion of a normally biallelic trinucleotide repeat in spinocerebellar ataxia type 2. *Nat Genet* 14: 269-276, 1996.
6. Orimo S, Ozawa E, Nakade S, Sugimoto T, Mizusawa H. <sup>123</sup>I-metaiodobenzylguanidine myocardial scintigraphy in Parkinson's disease. *J Neurol Neurosurg Psychiatry* 67: 189-194, 1999.
7. Infante J, Berciano J, Volpini V, et al. Spinocerebellar ataxia type 2 with levodopa-responsive parkinsonism culminating in motor neuron disease. *Mov Disord* 19: 848-852, 2004.
8. Sasaki H, Fukazawa T, Wakisaka A, et al. Central phenotype and related varieties of spinocerebellar ataxia type 2 (SCA2): a clinical and genetic study with a pedigree in the Japanese. *J Neurol Sci* 144: 176-181, 1996.
9. Estrada R, Galarraga J, Orozco G, Nodarse A, Auburger G. Spinocerebellar ataxia type 2 (SCA2): morphometric analyses in 11 autopsies. *Acta Neuropathol* 97: 306-310, 1999.
10. Kim JM, Hong S, Kim GP, et al. Importance of low-range CAG expansion and CAA interruption in SCA2 Parkinsonism. *Arch Neurol* 64: 1510-1518, 2007.
11. Charles P, Camuzat A, Benammar N, et al. Are interrupted SCA2 CAG repeat expansions responsible for parkinsonism? *Neurology* 69: 1970-1975, 2007.
12. Momeni P, Lu CS, Chou YW, et al. Taiwanese cases of SCA2 are derived from a single founder. *Mov Disord* 20: 1633-1636, 2005.
13. Sasaki H, Wakisaka A, Sanpei K, et al. Phenotype variation correlates with CAG repeat length in SCA2: a study of 28 Japanese patients. *J Neurol Sci* 159: 202-208, 1998.
14. Matsuura T, Sasaki H, Yabe I, et al. Mosaicism of unstable CAG repeats in the brain of spinocerebellar ataxia type 2. *J Neurol* 246: 835-839, 1999.
15. Elden AC, Kim HJ, Hart MP, et al. Ataxin-2 intermediate-length polyglutamine expansions are associated with increased risk for ALS. *Nature* 466: 1069-1075, 2010.

## Cerebrospinal Fluid Neopterin, but not Osteopontin, is a Valuable Biomarker for the Treatment Response in Patients with HTLV-I-associated Myelopathy

Masahiro Nagai, Tomoaki Tsujii, Hiroataka Iwaki, Noriko Nishikawa and Masahiro Nomoto

### Abstract

**Objective** The concentrations of neopterin and osteopontin in the cerebrospinal fluid (CSF) were measured in patients with HTLV-I-associated myelopathy/tropical spastic paraparesis (HAM/TSP) in order to evaluate their utility as biomarkers for the treatment response.

**Methods** Seven HAM/TSP patients were treated intravenously with high-dose methylprednisolone (1,000 mg/day) for 3 days. CSF samples were collected before and after the treatment. The neopterin and osteopontin concentrations were determined using high-performance liquid chromatography (HPLC) and an enzyme immunoassay, respectively. The clinical symptoms were evaluated using the Osame Motor Disability Score and the Urinary Disturbance Score.

**Results** Four out of the seven patients showed an improvement in motor function with the treatment, and were therefore classed as responders. The pre-treatment CSF neopterin concentration exceeded the upper limit of normal in all seven of the patients, and tended to be higher in treatment responders as compared to non-responders. The CSF neopterin concentration was reduced following treatment in all patients. The mean CSF neopterin concentration significantly ( $p < 0.01$ ) decreased following treatment by almost 60% (from  $124.1 \pm 79.9$  nmol/L to  $49.2 \pm 29.8$  nmol/L). The mean CSF osteopontin concentration was significantly ( $p < 0.01$ ) higher in the HAM/TSP patients in comparison to the 18 HTLV-1-seronegative patients who were designated as controls ( $9.54 \pm 4.53$  mg/L vs.  $3.72 \pm 3.04$  mg/L). No significant ( $p = 0.47$ ) reduction of the CSF osteopontin concentration was observed following the intravenous administration of high-dose methylprednisolone.

**Conclusion** These results indicate that the CSF neopterin concentration, but not the osteopontin concentration, is a potentially valuable biomarker for monitoring the treatment response in HAM/TSP patients. Furthermore, high pre-treatment CSF neopterin concentrations may be a predictive biomarker for a response to intravenous high-dose methylprednisolone therapy.

**Key words:** HTLV-I, HAM/TSP, cerebrospinal fluid, neopterin, osteopontin, methylprednisolone

(Intern Med 52: 2203-2208, 2013)

(DOI: 10.2169/internalmedicine.52.0869)

### Introduction

Human T-cell lymphotropic virus type I (HTLV-I) is an exogenous human retrovirus that has been demonstrated to be the etiological agent in adult T-cell leukemia as well as in a progressive neurological disease called HTLV-I-associated myelopathy/tropical spastic paraparesis (HAM/

TSP). The vast majority of HTLV-I-infected individuals are clinically asymptomatic, with <5% of infected individuals ever developing HAM/TSP. Clinically, HAM/TSP is characterized by muscle weakness, hyperreflexia, spasticity in the lower extremities and urinary disturbance associated with the preferential damage of the thoracic spinal cord (1). Although it is not yet completely understood how HTLV-I causes HAM/TSP, it is believed that increased HTLV-I

Department of Neurology and Clinical Pharmacology, Ehime University Graduate School of Medicine, Japan

Received for publication April 26, 2013; Accepted for publication June 2, 2013

Correspondence to Dr. Masahiro Nomoto, nomoto@m.ehime-u.ac.jp

**Table 1. Patient Characteristics**

Patient no.	Age (years)	Sex	Disease duration (years)	CSF anti-HTLV-I antibody titer
1	70	M	13	1:512
2	81	F	2	1:800
3	48	F	2	1:256
4	48	F	4	1:800
5	77	F	5	1:512
6	60	F	2	1:512
7	56	F	10	1:128

F: female, M: male

proviral loads and immune responses to HTLV-I infected cells play a pivotal role in the pathogenesis of this disorder (2).

Consequently, therapeutic strategies for HAM/TSP patients are directed towards these pathogenic phenomena. The first therapeutic strategy is to reduce HTLV-I loads, although anti-retroviral reagents such as reverse transcriptase inhibitors seem to be less effective for HTLV-I infections than for human immunodeficiency virus (HIV) infections. The second therapeutic strategy is to modulate the abnormal immune responses in HAM/TSP patients. Several immunosuppressive or immunomodulating therapies have been tried, including corticosteroids, interferon- $\alpha$  (IFN- $\alpha$ ), azathioprine and plasmapheresis (3). Chronic oral prednisolone therapy was empirically the most effective for the improvement of the neurological impairment that is associated with HAM/TSP. However, adverse events such as osteoporosis, glucose intolerance and gastroduodenal ulceration have limited its use for HAM/TSP patients, especially elderly postmenopausal women. We have chosen IV high-dose methylprednisolone as a first-line therapy because this treatment has a better tolerability profile than chronic oral prednisolone therapy. Another reason is because IV high-dose methylprednisolone therapy has been extensively and successfully used for patients with relapses of multiple sclerosis or other immune-mediated neurological disorders.

Although the anti-HTLV-I antibody titer in the cerebrospinal fluid (CSF) is used as a diagnostic biomarker of HAM/TSP, it is inadequate as a biomarker for monitoring the treatment response. However, increased CSF neopterin concentrations have been previously reported in patients with HAM/TSP (4, 5). Neopterin is a pyrazino-pyrimidine compound that is produced by macrophages after stimulation by IFN- $\gamma$  from activated T cells. The concentration of neopterin in the CSF has been used as a biomarker for cellular immune response in the central nervous system (CNS). Osteopontin has multiple functions and is involved in the recruitment of macrophage and T cells in inflammatory lesions. Osteopontin enhances IFN- $\gamma$  and interleukin (IL)-12 production and depresses the release of IL-10 from immune cells (6). It is up-regulated in the brains of patients with multiple sclerosis and in the spinal cords of mice with experimental autoimmune encephalomyelitis (7, 8). It is therefore believed that both neopterin and osteopontin could be valuable biomarkers for indicating the severity of inflamma-

**Table 2. Rating Scale for the Osame Motor Disability Score**

0	Normal walking and running
1	Normal gait but runs slowly
2	Abnormal gait
3	Abnormal gait and unable to run
4	Needs support while using stairs
5	Needs 1-hand support in walking
6	Needs 2-hand support in walking
7	Needs 2-hand support in walking and is limited to 10 m
8	Needs 2-hand support in walking and is limited to 5 m
9	Unable to walk but able to crawl on hands and knees
10	Crawls with hands
11	Unable to crawl but can turn sideways in bed
12	Unable to turn sideways but can move toes
13	Completely bedridden

tion and the degree of T cell activation in the CNS.

Chronic oral prednisolone therapy decreases CSF neopterin concentrations in HAM/TSP patients (3). However, it is not yet known if CSF neopterin concentrations change rapidly after treatment and might, therefore, be useful in predicting the response to corticosteroid therapy. The CSF osteopontin concentrations in HAM/TSP patients have not yet been investigated. We herein present the results of our study in which we monitored the CSF neopterin and osteopontin concentrations before and after IV high-dose methylprednisolone therapy in patients with HAM/TSP in order to evaluate their utility as biomarkers for treatment response.

## Materials and Methods

The diagnosis of HAM/TSP was made according to the current WHO diagnosis guidelines. The anti-HTLV-I antibody titers were measured using a particle-agglutination (PA) test. The characteristics of the seven patients with HAM/TSP who were recruited are summarized in Table 1. They had not been previously treated with either immunosuppressive or immunomodulating agents. They were treated with IV infusions of high-dose methylprednisolone (1,000 mg/day) for 3 days following their hospital admission. None of the patients received any additional oral corticosteroid therapy following the IV administration of high-dose methylprednisolone. The Osame Motor Disability Score (OMDS) and the Urinary Disturbance Score (UDS) were used for the clinical evaluation. The OMDS rating scale is shown in Table 2. The UDS was calculated from the sum of the scores (0=normal, 1=slight, 2=moderate, 3=severe) for three symptoms (increased frequency of urination, feeling of residual urine, incontinence). CSF was obtained from each patient with written informed consent. Lumbar punctures were performed before and within 7 days of treatment completion. The collected CSF was stored at  $-80^{\circ}\text{C}$  until analyzed. The study was approved by the hospital ethics committee.

The CSF neopterin concentrations were measured using high-performance liquid chromatography (HPLC) with fluorometric detection. Thawed CSF aliquots (100  $\mu\text{L}$ ) were acidified with ice-cold 0.1 M HCl (100  $\mu\text{L}$ ) and kept on ice.



A mixture of 1% I<sub>2</sub> and 2% KI in 0.1 M HCl (50 µL) was then added, and the samples were incubated at room temperature under dark conditions. An aqueous solution of 1.5% ascorbic acid (50 µL) was then added to the mixture, which was then centrifuged at 10,000 rpm for 1 min. The supernatant (100 µL) was injected into a C18 column (150×2.1 mm) with 3.5% methanol in water as the mobile phase. The quantification of osteopontin in the CSF samples was performed using a commercially available enzyme immunoassay kit (human osteopontin assay kit, Immunobiological Laboratories, Japan) according to the manufacturer's protocol.

Statistical analysis was performed using the JMP10 software program (SAS). The results are expressed as mean±SD and median values. The paired data from before and after treatment were analyzed by Wilcoxon's signed-rank test. The Mann-Whitney U test was used to compare groups. p values of <0.05 were considered to be statistically significant.

### Results

Four out of the seven patients showed improvement in their motor function after treatment with IV high-dose methylprednisolone. One patient improved by two grades and the

others improved by one grade on the OMDS rating scale (Table 3). An improvement in the urinary disturbance score was observed in four patients (Table 3). Three of the patients showed improvements on both scales, while one patient showed an improvement in the urinary disturbance score without an associated improvement in motor function and a second patient showed improved motor function without an improvement in the urinary disturbance score. Five patients had sensory disturbance (pain and numbness of lower limbs and back pain) before the treatment. The treatment alleviated pain in all five patients.

The CSF neopterin concentrations exceeded the upper limit of normal (30 nmol/L) in all of the patients before treatment. The mean CSF neopterin concentration was 124.1±79.9 nmol/L (median 89.9 nmol/L) for all seven patients prior to treatment. The CSF neopterin concentrations decreased in all of the patients after IV high-dose methylprednisolone therapy. The mean CSF neopterin concentration was significantly (p<0.01) reduced by almost 60% after treatment to 49.2±29.8 nmol/L (median: 43.4 nmol/L) (Table 4). The changes in the CSF neopterin concentrations according to the treatment parameters for each patient are shown in Fig. 1.

**Table 3. Changes in the Disability Scores after IV High-dose Methylprednisolone Therapy**

Patient no.	OMDS		UDS	
	Before	After	Before	After
1	5	4	6	5
2	10	8	9	7
3	4	4	5	3
4	3	3	3	3
5	5	4	3	3
6	10	9	7	6
7	5	5	3	3

OMDS: Osame Motor Disability Score, UDS: Urinary Disturbance Score

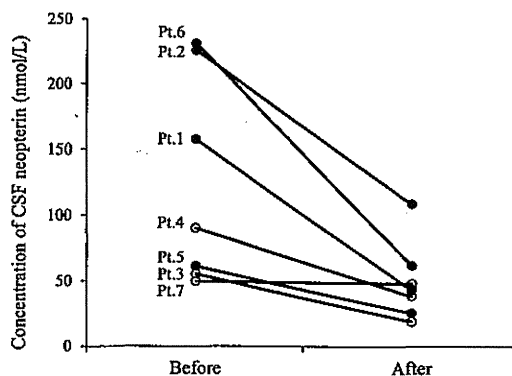


**Figure 1. The CSF neopterin concentrations before and after IV high-dose methylprednisolone therapy. The closed and open symbols indicate clinical responders and non-responders, respectively.**

**Table 4. Changes in the CSF Parameters after IV High-dose Methylprednisolone Therapy**

Patient no.	Neopterin (nmol/L)		Osteopontin (mg/L)		anti-HTLV-I antibody titer		Cells (µL)		Protein (mg/dL)	
	Before	After	Before	After	Before	After	Before	After	Before	After
1	157.4	43.4	10.69	13.46	1:512	1:512	6	2	25	27
2	225.5	108.7	7.22	9.36	1:800	1:256	10	8	54	50
3	54.9	18.9	3.67	5.05	1:256	1:128	6	7	45	29
4	89.9	38.5	13.15	12.33	1:800	1:800	7	6	50	44
5	60.9	25.4	4.66	4.81	1:512	1:128	3	3	39	35
6	230.8	61.7	16.02	11.50	1:512	1:512	12	6	52	29
7	49.5	47.8	11.36	3.70	1:128	1:256	5	7	20	23

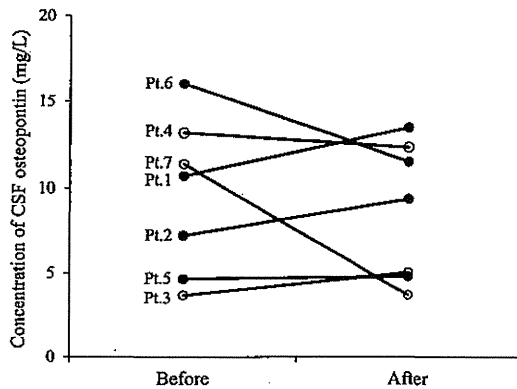


**Figure 2.** The CSF osteopontin concentrations before and after IV high-dose methylprednisolone therapy. The closed and open symbols indicate clinical responders and non-responders, respectively.

The mean CSF osteopontin concentration was  $9.54 \pm 4.53$  mg/L (median 10.69 mg/L) prior to treatment. Unlike for neopterin, our laboratory had not yet set an upper limit of normal for CSF osteopontin. We therefore compared CSF osteopontin concentrations for our seven HAM/TSP patients to those for 18 HTLV-I-seronegative patients with spondylosis as a control group. The mean CSF osteopontin concentration was  $3.72 \pm 3.04$  mg/L (median 3.52 mg/L) in the control group. The pre-treatment CSF osteopontin concentration in our seven HAM/TSP patients was significantly ( $p < 0.01$ ) higher than that of the control group. The mean CSF osteopontin concentration was  $8.6 \pm 4.03$  mg/L (median: 9.36 mg/L) after treatment in the seven HAM/TSP patients, which was not significantly ( $p = 0.47$ ) different than the pre-treatment values (Table 4). The pre-treatment and post-treatment CSF osteopontin concentrations for each HAM/TSP patient are shown in Fig. 2.

We defined HAM/TSP patients who showed an OMS improvement as responders. The mean pre-treatment CSF neopterin concentration in responders ( $n = 4$ ) was  $168.7 \pm 79.2$  nmol/L (median 191.5 nmol/L), but only  $64.8 \pm 22.0$  nmol/L (median 54.9 nmol/L) in non-responders ( $n = 3$ ). While the pre-treatment CSF neopterin concentrations tended to be higher among responders compared to non-responders, the difference was not statistically significant ( $p = 0.056$ ). The mean pre-treatment CSF osteopontin concentration was  $9.64 \pm 4.91$  mg/L (median 8.95 mg/L) in responders and  $9.34 \pm 5.04$  mg/L (median 11.36 mg/L) in non-responders with no significant difference between the groups ( $p = 0.43$ ).

The HTLV-I antibody titer, and the number of cells and the amount of protein in the CSF were not significantly altered by the treatment (Table 4).

The IV high-dose methylprednisolone therapy was well tolerated by all of the patients. Although insomnia was observed as an adverse effect of treatment, it was transient. No serious adverse events were observed.

## Discussion

We herein demonstrate that the CSF neopterin concentration significantly decreases following IV high-dose methylprednisolone therapy in patients with HAM/TSP. While the pre-treatment CSF osteopontin concentrations were significantly higher in HAM/TSP patients as compared to the controls, there were no statistically significant changes in the CSF osteopontin concentrations after treatment.

The coexistence of a high HTLV-I proviral load and HTLV-I-specific T cells is an important feature of HAM/TSP (9). This distinguishing feature is observed in both peripheral blood and CSF of patients with HAM/TSP (9, 10). Histopathological studies indicate the existence of HTLV-I-infected cells as well as a local inflammatory response in the spinal cord lesions of HAM/TSP patients (11, 12). It is therefore believed that the immune response to HTLV-I likely contributes to the inflammatory process of the CNS lesions in HAM/TSP patients and causes the clinical symptoms of HAM/TSP. Activated lymphocytes and macrophages up-regulate the production of pro-inflammatory cytokines such as IL-1, IL-6 and IFN- $\gamma$  (13). The significant elevation of the levels of these cytokines has been described in the CSF of HAM/TSP patients (14, 15). High values of CSF neopterin have also been reported in HAM/TSP patients (4, 5). Neopterin is released by stimulated macrophages, and the concentration of CSF neopterin reflects the degree of the inflammatory response in the CNS. The concentration of CSF neopterin is significantly correlated with the HTLV-I proviral load, which is an important risk factor for the development of HAM/TSP (10). The CSF neopterin concentration is therefore useful as an adjunct to the diagnosis of HAM/TSP. In our study, we confirmed the elevation of CSF neopterin concentrations in HAM/TSP patients.

Moreover, we also demonstrated that CSF osteopontin concentrations are increased in HAM/TSP patients. To the best of our knowledge, this is the first report concerning osteopontin concentrations in HAM/TSP patients. Osteopontin is a secreted phosphoprotein that is produced by many kinds of cells including osteoblasts, activated lymphocytes, macrophages, vascular smooth muscle cells and kidney cells (16). It has a multifunctional capacity, and is involved in bone remodeling, tumor progression, atherosclerosis, inflammation and immunity (16). Osteopontin promotes the production of pro-inflammatory cytokines such as IL-12 and IFN- $\gamma$  (6). Several studies have reported that osteopontin concentrations are significantly elevated in the CSF of patients with multiple sclerosis (17-19). Our finding suggests that a chronic inflammatory response in the CNS lesions of HAM/TSP is reflected by the CSF osteopontin concentrations as well as the CSF neopterin concentrations. If so, which is the better diagnostic marker for HAM/TSP? The CSF neopterin concentrations exceeded the upper limit of normal in all HAM/TSP patients. However, the CSF osteopontin concentrations in three of the seven HAM/TSP patients overlapped the range

measured for the control group. Thus, the CSF neopterin concentration would appear to be more suitable for discriminating HAM/TSP and non-HAM/TSP patients than CSF osteopontin concentration.

Various treatments have been tried for HAM/TSP patients (3). Almost all of the studies have been open-label trials or case series with the exception of a multicenter, randomized placebo-controlled, double-blind study of an IFN- $\alpha$  trial in Japan (20). However, no study has conclusively demonstrated a long-term clinical benefit. Well-designed clinical trials are therefore necessary in order to develop effective therapies which may improve the long-term prognoses for HAM/TSP patients (21). In addition, validated surrogate biomarkers are required for the determination of the effectiveness of investigational treatments.

It has been previously reported that approximately 70% of HAM/TSP patients who are treated with a chronic oral administration of prednisolone ( $n=131$ ) improved by at least one OMDS grade (3). Furthermore, the treatment significantly decreased the reported CSF neopterin concentrations in 16 patients. The mean CSF neopterin concentration was also reduced from 155.4 nmol/L to 79.5 nmol/L by IV high-dose methylprednisolone therapy in eight of the previously reported patients, but the change was not statistically significant (3). Unfortunately, the timing of the CSF sampling after IV high-dose methylprednisolone therapy was not specified in that publication. The timing of CSF sampling is likely critical with such short-term therapies as IV high-dose methylprednisolone, since the CSF neopterin concentration seems to increase after the discontinuation of treatment. In our study, the CSF samples were collected within 7 days of the completion of the IV high-dose methylprednisolone therapy in order to attenuate the impact of the change on the CSF neopterin concentration. The CSF neopterin concentration changed rapidly after IV high-dose methylprednisolone therapy. This finding suggests that CSF neopterin is a sensitive biomarker for the evaluation of the early-phase response to treatments in HAM/TSP patients. This feature may be partially due to the short half-life of neopterin which has been estimated to be 90 minutes in the circulation (22). In contrast, there was no significant change in the CSF osteopontin concentrations that were observed after IV high-dose methylprednisolone therapy in the HAM/TSP patients. Even though there is a possibility that a change in the CSF osteopontin concentration may arise several days after the treatment, it is clear that the CSF osteopontin concentration is unreliable as a biomarker for the assessment of an early-phase response to treatment. Although the influence of IV high-dose methylprednisolone therapy on HTLV-I proviral loads is still unclear, the therapy doesn't seem to reduce HTLV-I proviral loads. It has been reported that the osteopontin gene was transactivated by HTLV-I Tax protein (23). If the elevation of the CSF osteopontin levels in HAM/TSP patients is due to an HTLV-I infection of the osteopontin producing cells, but not the inflammatory response, then the unchanged osteopontin levels by IV high-dose methylpredni-

solone therapy are thus thought to be understandable.

Although it was not a statistically significant difference, and it is most likely due to the small number of patients, the pre-treatment CSF neopterin concentrations of those patients who responded to the IV high-dose methylprednisolone therapy tended to be higher than those of non-responders. This suggests that patients with relatively high values of CSF neopterin may have a more favorable response to IV high-dose methylprednisolone therapy. Additional patients need to be examined in order to confirm the belief that CSF neopterin is useful as a predictive biomarker for responders to IV high-dose methylprednisolone therapy.

The mechanism of action of for the corticosteroids on HAM/TSP remains to be elucidated. The anti-inflammatory properties of the corticosteroids may attenuate the degree of the inflammatory response in spinal cord lesions. This non-specific anti-inflammatory effect may result in clinical improvements in the patients, especially when the inflammation is very intense. Moreover, corticosteroids may also affect the HTLV-I infected cells or the immune response to HTLV-I. It has been demonstrated that betamethasone therapy decreased CD4<sup>+</sup>Tax<sup>+</sup> T cells and increased CD4<sup>+</sup>Foxp3<sup>+</sup> T cells (regulatory T cells) in the peripheral blood samples of patients with HAM/TSP (24). Corticosteroids therapy may reduce the erratic IFN- $\gamma$  production by T-cells in patients with HAM/TSP, which is then followed by a reduction of neopterin release by the stimulated macrophages.

Our study did not address how long the clinical effect and the reduction of CSF neopterin concentration lasted after the IV high-dose methylprednisolone therapy had been discontinued. An open-label clinical trial of IV high-dose methylprednisolone has been reported from Brazil, in which 39 patients with HAM/TSP received IV high-dose methylprednisolone every 3-4 months (25). The Incapacity Status Scale showed a significant neurological improvement of 24.5% after a mean follow-up of 2.2 years. However, the CSF biomarkers were not reported in that trial. Further study will therefore be needed to clarify the long-term changes in the CSF neopterin concentration following the treatment of HAM/TSP patients.

In conclusion, our results indicate that the concentration of CSF neopterin, but not that of osteopontin, is a potentially valuable biomarker for monitoring treatment response in HAM/TSP patients. In addition, high pre-treatment CSF neopterin concentrations may be a predictive biomarker for response to IV high-dose methylprednisolone therapy.

**The authors state that they have no Conflict of Interest (COI).**

#### Acknowledgement

This study was supported by Grant-in-Aids for Orphan and Neurodegenerative Disorders from the Ministry of Health, Labour and Welfare, GJTS, and a Grant of Ehime University. The authors wish to thank Ms. Madoka Kubo for her excellent technical assistance.

## References

1. Osame M, Usuku K, Izumo S, et al. HTLV-I associated myelopathy, a new clinical entity. *Lancet* **1**: 1031-1032, 1986.
2. Nagai M, Osame M. Human T-cell lymphotropic virus type I and neurological diseases. *J Neurovirol* **9**: 228-235, 2003.
3. Nakagawa M, Nakahara K, Maruyama Y, et al. Therapeutic trials in 200 patients with HTLV-I-associated myelopathy/tropical spastic paraparesis. *J Neurovirol* **2**: 345-355, 1996.
4. Nomoto M, Utatsu Y, Soejima Y, Osame M. Neopterin in cerebrospinal fluid: a useful marker for diagnosis of HTLV-I-associated myelopathy/tropical spastic paraparesis. *Neurology* **41**: 457, 1991.
5. Ali A, Rudge P, Dalgleish AG. Neopterin concentrations in serum and cerebrospinal fluid in HTLV-I infected individuals. *J Neurol* **239**: 270-272, 1992.
6. Ashkar S, Weber GF, Panoutsakopoulou V, et al. Eta-1 (osteopontin): an early component of type-1 (cell-mediated) immunity. *Science* **287**: 860-864, 2000.
7. Chabas D, Baranzini SE, Mitchell D, et al. The influence of the proinflammatory cytokine, osteopontin, on autoimmune demyelinating disease. *Science* **294**: 1731-1735, 2001.
8. Braitch M, Constantinescu CS. The role of osteopontin in experimental autoimmune encephalomyelitis (EAE) and multiple sclerosis (MS). *Inflamm Allergy Drug Targets* **9**: 249-256, 2010.
9. Nagai M, Yamano Y, Brennan MB, Mora CA, Jacobson S. Increased HTLV-I proviral load and preferential expansion of HTLV-I Tax-specific CD8<sup>+</sup> T cells in cerebrospinal fluid from patients with HAM/TSP. *Ann Neurol* **50**: 807-812, 2001.
10. Nagai M, Usuku K, Matsumoto W, et al. Analysis of HTLV-I proviral load in 202 HAM/TSP patients and 243 asymptomatic HTLV-I carriers: high proviral load strongly predisposes to HAM/TSP. *J Neurovirol* **4**: 586-593, 1998.
11. Matsuoka E, Takenouchi N, Hashimoto K, et al. Perivascular T cells are infected with HTLV-I in the spinal cord lesions with HTLV-I-associated myelopathy/tropical spastic paraparesis: double staining of immunohistochemistry and polymerase chain reaction in situ hybridization. *Acta Neuropathol* **96**: 340-346, 1998.
12. Umehara F, Izumo S, Nakagawa M, et al. Immunocytochemical analysis of the cellular infiltrate in the spinal cord lesions in HTLV-I-associated myelopathy. *J Neuropathol Exp Neurol* **52**: 424-430, 1993.
13. Umehara F, Izumo S, Ronquillo AT, Matsumuro K, Sato E, Osame M. Cytokine expression in the spinal cord lesions in HTLV-I-associated myelopathy. *J Neuropathol Exp Neurol* **53**: 72-77, 1994.
14. Nishimoto N, Yoshizaki K, Eiraku N, et al. Elevated levels of interleukin-6 in serum and cerebrospinal fluid of HTLV-I-associated myelopathy/tropical spastic paraparesis. *J Neurol Sci* **97**: 183-193, 1990.
15. Furuya T, Nakamura T, Fujimoto T, et al. Elevated levels of interleukin-12 and interferon-gamma in patients with human T lymphotropic virus type I-associated myelopathy. *J Neuroimmunol* **95**: 185-189, 1999.
16. Denhardt DT, Guo X. Osteopontin: a protein with diverse functions. *FASEB J* **7**: 1475-1482, 1993.
17. Braitch M, Nunan R, Niepel G, Edwards LJ, Constantinescu CS. Increased osteopontin levels in the cerebrospinal fluid of patients with multiple sclerosis. *Arch Neurol* **65**: 633-635, 2008.
18. Bornsen L, Khademi M, Olsson T, Sorensen PS, Sellebjerg F. Osteopontin concentrations are increased in cerebrospinal fluid during attacks of multiple sclerosis. *Mult Scler* **17**: 32-42, 2011.
19. Wen SR, Liu GJ, Feng RN, et al. Increased levels of IL-23 and osteopontin in serum and cerebrospinal fluid of multiple sclerosis patients. *J Neuroimmunol* **244**: 94-96, 2012.
20. Izumo S, Goto I, Itoyama Y, et al. Interferon-alpha is effective in HTLV-I-associated myelopathy: a multicenter, randomized, double-blind, controlled trial. *Neurology* **46**: 1016-1021, 1996.
21. Yamano Y, Sato T. Clinical pathophysiology of human T-lymphotropic virus-type I-associated myelopathy/tropical spastic paraparesis. *Front Microbiol* **3**: 389, 2012.
22. Fuchs D, Stahl-Hennig C, Gruber A, et al. Neopterin: its clinical use in urinalysis. *Kidney Int Suppl* **47**: S8-S11, 1994.
23. Zhang J, Yamada O, Matsushita Y, et al. Transactivation of human osteopontin promoter by human T-cell leukemia virus type I-encoded Tax protein. *Leuk Res* **34**: 763-768, 2010.
24. Alberti C, Cartier L, Valenzuela MA, Puente J, Tanaka Y, Ramirez E. Molecular and clinical effects of betamethasone in human T-cell lymphotropic virus type-I-associated myelopathy/tropical spastic paraparesis patients. *J Med Virol* **83**: 1641-1649, 2011.
25. Croda MG, de Oliveira AC, Vergara MP, et al. Corticosteroid therapy in TSP/HAM patients: the results from a 10 years open cohort. *J Neurol Sci* **269**: 133-137, 2008.

## ORIGINAL ARTICLE

## Histopathological differences between human T-lymphotropic virus type 1-positive and human T-lymphotropic virus type 1-negative polymyositis

Hazem M. Abdullah,<sup>1,2</sup> Itsuro Higuchi,<sup>3</sup> Ryuji Kubota,<sup>1</sup> Eiji Matsuura,<sup>3</sup> Akihiro Hashiguchi,<sup>3</sup> Nashwa H. Abdelbary,<sup>1</sup> Yukie Inamori,<sup>3</sup> Hiroshi Takashima<sup>3</sup> and Shuji Izumo<sup>1</sup>

<sup>1</sup>Division of Molecular Pathology, Center for Chronic Viral Diseases, Kagoshima City, Japan, <sup>2</sup>Department of Human Pathology, Faculty of Medicine, Mansoura University, Mansoura City, Dakahlia Governorate, Egypt, and <sup>3</sup>Department of Neurology and Geriatrics, Graduate School of Medical and Dental Sciences, Kagoshima University, Kagoshima City, Japan

### Keywords

cytochrome c oxidase; human T-lymphotropic virus type 1; mitochondrial abnormality; polymyositis

### Correspondence

Shuji Izumo MD, PhD, Division of Molecular Pathology, Center for Chronic Viral Diseases, Graduate School of Medical and Dental Sciences, Kagoshima University, 8-35-1 Sakuragaoka, Kagoshima City 890-8544, Japan.  
Tel: +81-99-275-5940  
Fax: +81-99-275-5942  
Email: izumo@m.kufm.kagoshima-u.ac.jp

Received: 1 October 2010; revised: 7 December 2010; accepted: 19 December 2010.

### Abstract

**Objectives:** Epidemiological studies show that human T-lymphotropic virus type 1 (HTLV-1) is closely associated with polymyositis (PM). However, the pathogenic roles of HTLV-1 in PM remain unknown. The present study aims to assess skeletal muscle morphology in the presence of HTLV-1 infection to compare the histopathological findings of HTLV-1-positive and HTLV-1-negative PM.

**Methods:** Among the 68 patients with inflammatory myopathy diagnosed through muscle biopsy over the previous 10 years at Kagoshima University Hospital, we retrospectively selected 21 patients with PM not associated with any other disease; we evaluated HTLV-1 positivity through serology, confirmed it by nested polymerase chain reaction using DNA extracted from muscles, and then assessed the tissue viral load. Meticulous histopathological examination was carried out using routine histochemical and immunohistochemical staining, and specimens from selected cases were examined by electron microscopy.

**Results:** The clinical and histopathological findings of muscle biopsy specimens of HTLV-1-positive ( $n = 11$ ) and HTLV-1-negative PM cases ( $n = 10$ ) were compared. Compared with HTLV-1-negative patients, HTLV-1-positive patients showed protracted clinical courses, prominent endomysial infiltrates, infrequent necrotic fibers and prominent regenerative activities. Furthermore, they showed frequent cytochrome c oxidase deficiency and ultrastructural abnormalities in mitochondria.

**Conclusions:** These differences are significant, but not specific to HTLV-1-positive PM. Therefore, HTLV-1 might induce the clinical and histopathological modifications of PM observed in the present study. (Clin. Exp. Neuroimmunol. doi: 10.1111/j.1759-1961.2011.00017.x, January 2011)

### Introduction

Human T-lymphotropic virus type 1 (HTLV-1), the first human retrovirus to be identified, is a causative agent of adult T-cell leukemia (ATL). HTLV-1 has been reported to be associated with a particular type of chronic progressive myelopathy: HTLV-1-associated myelopathy/tropical spastic paresis (HAM/TSP).<sup>1</sup> HTLV-1 infection has also been linked to

other inflammatory diseases, such as uveitis, arthritis, bronchoalveolitis, Sjögren's syndrome and myositis.<sup>2</sup> Epidemiological studies show a high incidence of seropositivity for HTLV-1 among polymyositis (PM) patients. However, whether HTLV-1 is a direct causative agent or it plays a role in the pathogenesis of PM remains unknown.<sup>2,3</sup> In addition, HTLV-1 infection is closely related to inclusion body myositis (IBM).<sup>4–6</sup>

PM and IBM are two types of inflammatory myopathies. IBM can be distinguished from PM by the presence of rimmed vacuoles, cytoplasmic inclusions and amyloid deposits in addition to inflammatory changes. However, because of the large similarity between PM and early IBM, modified criteria for diagnosis were introduced by Dalakas and Hohlfeld in 2003, in which careful follow up and repeated biopsies are required to avoid misdiagnosing early IBM as PM.<sup>7,8</sup>

To determine the clinical and histopathological differences between HTLV-1-positive and HTLV-1-negative PM, we retrospectively evaluated patients with PM not associated with any other disease and carried out a comparative study.

**Methods**

**Patients**

Of all patients who underwent muscle biopsy during the past 10 years at Kagoshima University Hospital, South Kyushu, Japan, 68 patients were reported to be diagnosed with inflammatory myopathy; of these patients, 21 were carefully selected for the present study, as shown in Fig. 1.

The 21 selected patients were re-evaluated using the modified criteria introduced by Dalakas and

Hohlfeld,<sup>7</sup> which list the following essential requirements for diagnosing PM: (i) elevated serum creatine kinase (CK); (ii) electromyography (EMG) abnormalities; and (iii) muscle biopsy abnormalities. Muscle biopsy abnormalities are crucial and include degeneration, regeneration, necrosis and foci of lymphocytic inflammatory cells with primary inflammation [i.e. CD8<sup>+</sup> cells surrounding healthy intact non-necrotic muscle fibers expressing major histocompatibility complex (MHC)-1 without rimmed vacuoles].

Informed consent was obtained from all patients. The institutional review board for regulating clinical research approved the present study.

**Muscle biopsy**

All muscle biopsies were obtained by open surgical procedures from the biceps brachii or quadriceps femoris. Muscle specimens for histopathological examination were snap-frozen by isopentane chilled in liquid nitrogen; 7-µm-thick sections were routinely stained with hematoxylin and eosin (HE), modified Gomori trichrome, periodic acid-Schiff (PAS), Sudan black, myosin ATPase, NADH-tetrazolium reductase, cytochrome c oxidase (CCO), adenosine monophosphate (AMP) deaminase, acid phosphatase and succinate dehydrogenase (SDH).<sup>9</sup> Select sections were

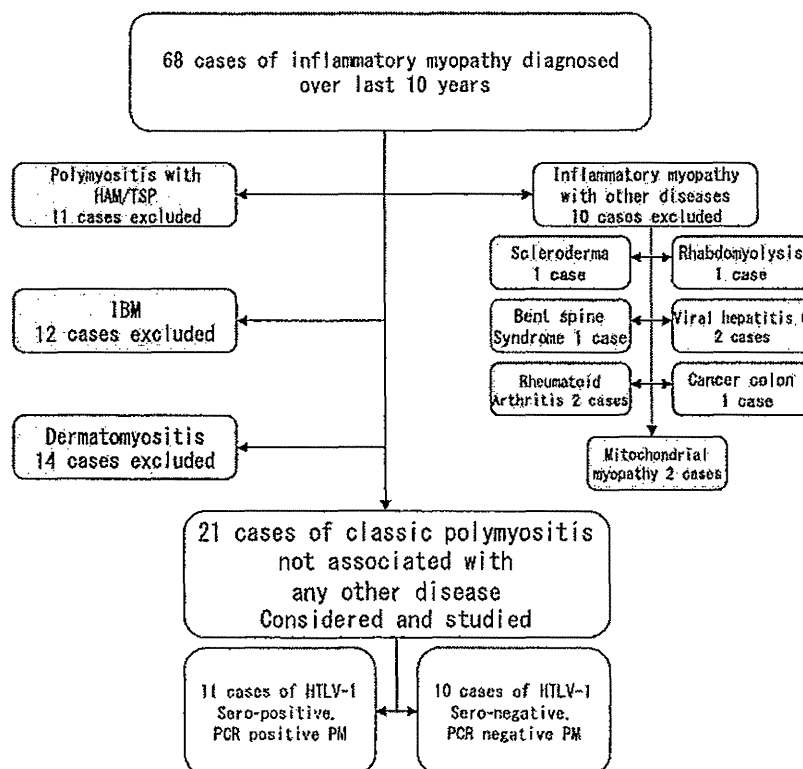


**Figure 1** Classification of final diagnoses after the initial diagnosis. The subjects reported with diagnoses other than polymyositis (PM) or PM associated with any other disease were excluded from further analysis. HAM/TSP, human T-lymphotropic virus type 1; HTLV-1, human T-lymphotropic virus type 1-associated myelopathy/tropical spastic paresis; IBM, inclusion body myositis; PCR, polymerase chain reaction.

immunohistochemically stained (e.g., with dysferlin or dystrophin) to exclude other suspected disorders.

#### Immunofluorescence double staining for CD8 and MHC-1

Frozen biopsied muscle specimens from all patients were cut into 7- $\mu$ m-thick sections, placed on aminosilane-coated slides and dried at room temperature. Sections were blocked with 10% normal goat serum in phosphate-buffered saline and then incubated with a mixture of mouse antihuman CD8 monoclonal antibody (diluted 1:50, isotype IgG1; Dako, Glostrup, Denmark) and mouse antihuman HLA-ABC antigen monoclonal antibody (diluted 1:50 isotype IgG2a; Dako) for 12 h at 4°C. Then, an isotype-specific goat antimouse antibody mixture (goat antimouse IgG1 Alexa Fluor 594 and goat antimouse IgG2a Alexa Fluor 488 to detect CD8 and HLA-ABC antigens, respectively; Invitrogen, Carlsbad, CA, USA) was applied for 60 min at room temperature. Sections were counterstained with 4',6-diamino-2-phenylindole. Signals were collected by a confocal laser scanning microscope (FV500; Olympus, Tokyo, Japan). The fluorescence of individual fluorochromes was captured sequentially.

#### Polymerase chain reaction

Polymerase chain reaction (PCR) was carried out in a Gene Amp PCR system 9700 (GeneAmp® Applied Biosystems, Singapore) to determine HTLV-1 positivity using 5  $\mu$ L of DNA (10  $\mu$ g/mL) extracted from fresh frozen muscle tissue as a template with 20  $\mu$ L of PCR mixture containing primers specific to the HTLV-1 pX region. Products were analyzed by electrophoresis using agarose gel, as described previously.<sup>10</sup>

The PCR products of samples that were not proven to be HTLV-1-positive were subjected to a second PCR under the same conditions and re-analyzed by electrophoresis using agarose gel. Samples that proved to be HTLV-1-positive after the second PCR were considered positive; samples that were HTLV-1-negative were subjected to the first PCR again, and the total amount of first PCR products (25  $\mu$ L) was subjected to a second PCR (5  $\mu$ L/reaction; i.e., five PCR reactions) to avoid loss of any viral amplicons. The results were reconsidered to be either positive or negative. All experiments were carried out using positive and negative controls, and sensitivity was determined by known titrated pX amplicon solutions from 1–5000 copies/5  $\mu$ L<sup>-1</sup>; the detection limit of the pX was one copy/reaction. All results were confirmed three times.

#### Real-time PCR

All cases that proved to be HTLV-1-positive were tested for tissue proviral load using an ABI PRISM7700 sequence detector (Applied Biosystems, Tokyo, Japan) using 15  $\mu$ L of DNA (10  $\mu$ g/mL) extracted from fresh frozen muscle tissue as a template with  $\beta$ -globin as an internal control. Tissue proviral loads were calculated using the following formula: (copy number of HTLV-1 Tax/10 000 cells) = [(tax average  $\times$  2)/ $\beta$ -actin average]  $\times$  10 000.<sup>11</sup> All samples were measured in triplicate, and the average was then determined.

#### Serology

HTLV-1 seropositivity was examined using a particle agglutinin method (Serodia-HTLV-1; Fujirebio, Tokyo, Japan) and an enzyme-linked immunosorbent assay (Virus-Antibody EIA IgG; Denka-Seiken, Japan).

#### Immunohistochemistry

Frozen biopsied muscle specimens from all patients were cut into 7- $\mu$ m-thick sections that were placed on aminosilane-coated slides, dried at room temperature and blocked with a blocking solution. The sections were then incubated with the following antibodies: monoclonal mouse antihuman CD4 (diluted 1:20), CD8 (diluted 1:50), CD20 (diluted 1:200) and CD68 (diluted 1:100; all obtained from Dako); neural cell adhesion molecule (NCAM; diluted 1:10; BD, Franklin Lakes, NJ, USA); myosin heavy chain (neonatal; MHCn; diluted 1:10; Novocastra, Newcastle, UK); perforin (diluted 1:25; PharmaCell, Paris, France); thrombomodulin (TM; diluted 1:50; Dako); and heat shock protein 47 (HSP47; diluted 1:50; Santa Cruz Biotechnology, Santa Cruz, CA, USA). Sections were incubated with each antibody for 12 h at 4°C. Antimouse antibodies were subsequently applied for 30 min at room temperature. Finally, the sections were visualized using the DAB (brown color) or DAKO AEC systems (red color) after setting positive and negative controls using mouse IgG negative control as a first antibody (Dako). Three control muscle biopsies that were HTLV-1-negative and had minimal pathological changes were also investigated.

#### Quantitative analysis of histopathological findings

Necrotic fibers, as well as all histochemical and immunohistochemical stains, were subjected to quantitative analysis. Samples (at least three sections from

each sample) were examined at five fields ( $\times 200$  magnification) selected randomly in a zigzag manner to avoid overlapping of the fields or recounting the same fibers. More than 200 fibers in each field were counted and all examined fields were averaged.

Each cellular subset and the total number of endomysial and perimysial infiltrating inflammatory cells were counted in at least three sections from each specimen at five different fields ( $\times 200$  magnification) selected randomly in a zigzag manner; the mean ratio of the total number of infiltrating inflammatory cells and each cellular subset was evaluated in all specimens of both groups.

#### Electron microscopy

Several epon-embedded tissue blocks from each of the seven HTLV-1-positive patients, five HTLV-1-negative PM patients and three normal control specimens were examined. Tissue blocks were fixed overnight in 3% glutaraldehyde, postfixed in 1% osmium tetroxide in 0.05 mol/L cacodylate buffer (pH 7.3), and dehydrated in graded alcohol. Semi-thin sections were stained with toluidine blue and safranin, and examined by light microscopy. Areas with inflammatory infiltrates and variable-sized fibers that were well fixed and free of preparation artifacts were selected for electron microscopy. Ultrathin sections were stained with uranyl acetate and lead citrate, and examined using an H-7100 electron microscope (Hitachi High-Technologies, Hitachinaka, Ibaraki, Japan). At least three tissue blocks from each specimen were cut, and at least three sections from each block were examined; five adjacent fibers in each field from five fields ( $\times 200$  magnification) selected randomly in a zigzag manner from each section were examined. More than 100 mitochondria in each fiber were counted, and the percentage was determined.

#### Statistical analysis

All quantitative data were analyzed for descriptive statistics and by the Mann-Whitney *U*-test and Spearman's rank correlation test using StatView software version 5.0.1. (SAS Institute Inc, Cary, NC, USA).

Data are presented as means (SD). *P*-values  $< 0.05$  were considered significant.

## Results

#### Patient selection

Of the 68 patients reported to have inflammatory myopathy who had undergone a biopsy over the

past 10 years, we carefully selected 21 patients with myositis not associated with skin lesions or any other diseases. Patients who reported to have dermatomyositis ( $n = 14$ ), IBM ( $n = 12$ ), inflammatory myopathy associated with HAM/TSP ( $n = 11$ ) and inflammatory myopathy associated with other diseases ( $n = 10$ ) were excluded from analysis on the basis of clinical and pathological criteria. The selection process and diagnoses of the excluded patients are shown in Fig. 1.

The 21 selected patients had the following common features: (i) subacute bilateral symmetrical progressive weakness commencing in adulthood and involving proximal muscles more than distal; (ii) elevated serum CK more than twice the normal level (normal range 26–140 IU/L); (iii) myopathic findings in EMG; and (iv) muscle biopsy findings (Fig. 2a–d,f) with inflammatory cell infiltration, CD8 cells surrounding healthy intact non-necrotic fibers as well as myopathic changes, such as variations in muscle fiber size, necrosis, degeneration and regeneration without rimmed vacuoles. In addition, the clinical course and manifestations of these 21 patients were retrospectively investigated to ensure a satisfactory response to steroid therapy with improvements in their symptoms (e.g., muscle tone, weakness and fatigue while walking, and lowered CK levels) and to confirm the diagnosis of PM.<sup>12,13</sup>

On re-evaluating the 21 selected PM patients using the modified criteria introduced by Dalakas and Hohlfeld,<sup>7</sup> the CD8/MHC-1 complex was detected in six patients (29%; Fig. 3a–c) who were diagnosed with definite PM. The remaining 15 patients showed MHC-1 expression and infiltration of CD8+ cells, but the CD8/MHC-1 complex was not detected; these patients were diagnosed with probable PM (Fig. 3d,f).

#### Confirmation of HTLV-1 positivity by nested PCR and proviral loads of HTLV-1-positive cases

Nested PCR carried out using DNA extracted from fresh frozen muscle biopsies showed that among the 21 patients with PM, 11 and 10 were HTLV-1-positive and HTLV-1-negative, respectively. PCR positivity for HTLV-1 strongly corresponded to seropositivity for HTLV-1. Although tissue proviral loads of HTLV-1 ranged from 1 to 2063 (1 copy/ $10^4$  cells), the proviral loads were not correlated with any examined clinical or histopathological values using Spearman's rank correlation test (data not shown).

The six patients expressing the CD8/MHC-1 complex included three from the HTLV-1 positive group



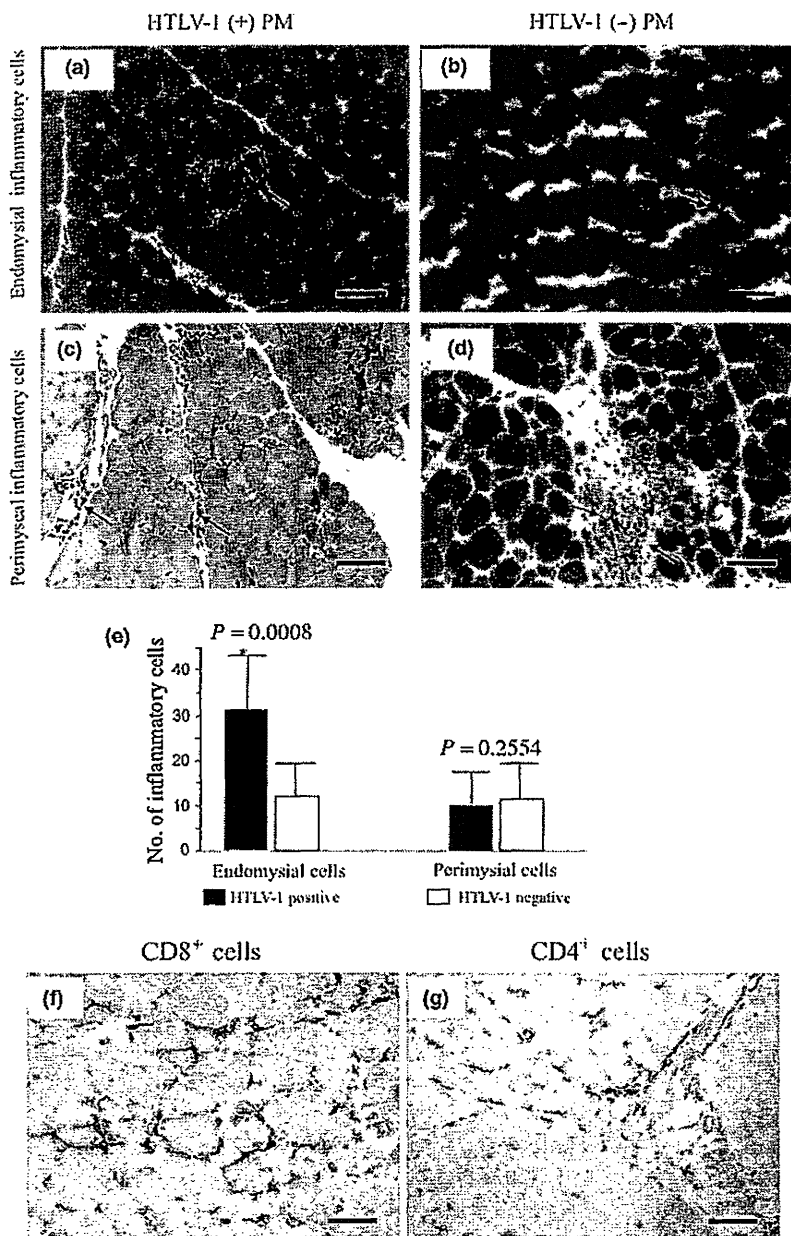


**Figure 2** Distribution and subsets of inflammatory cells in cross-sections of muscles biopsied from human T-lymphotropic virus type 1 (HTLV-1)-positive and HTLV-1-negative polymyositis (PM) patients. (a) Abundant endomysial inflammatory cells in HTLV-1-positive PM (arrow). (b) Infrequent endomysial inflammatory cells in HTLV-1-negative PM (arrows). (c,d) Equal numbers of perimysial inflammatory cells in HTLV-1-positive and HTLV-1-negative PM (arrows). Bars (a)–(d) 100  $\mu$ m. (e) Combined data for all study patients. Significantly greater numbers of endomysial inflammatory cells in HTLV-1-positive PM ( $P = 0.0008$ ; Mann-Whitney  $U$ -test). Immunohistochemistry for (f) CD8<sup>+</sup> (bar, 50  $\mu$ m) and (g) CD4<sup>+</sup> (bar, 100  $\mu$ m) cells shows that they are predominant in the endomysium and perimysium, respectively.

(3/11, 27%) and three from the HTLV-1-negative group (3/10, 30%).

**Clinical and laboratory differences**

Detailed clinical and laboratory data are shown in Table 1. There were no significant differences between groups regarding age, sex or serum CK levels. However, the duration of illness from the onset of symptoms to biopsy was significantly longer in HTLV-1-positive PM patients [range 1–240 months;

mean 66 months (73.6)] compared with that in HTLV-1-negative PM patients [range 1–24 months; mean 8 months (6.9);  $P = 0.0043$ ].

Endomysial inflammatory cells are more frequent in HTLV-1-positive PM

Routine examination showed typical histopathological findings of PM in all patients. However, there were significantly more endomysial inflammatory cells in HTLV-1-positive PM patients [range

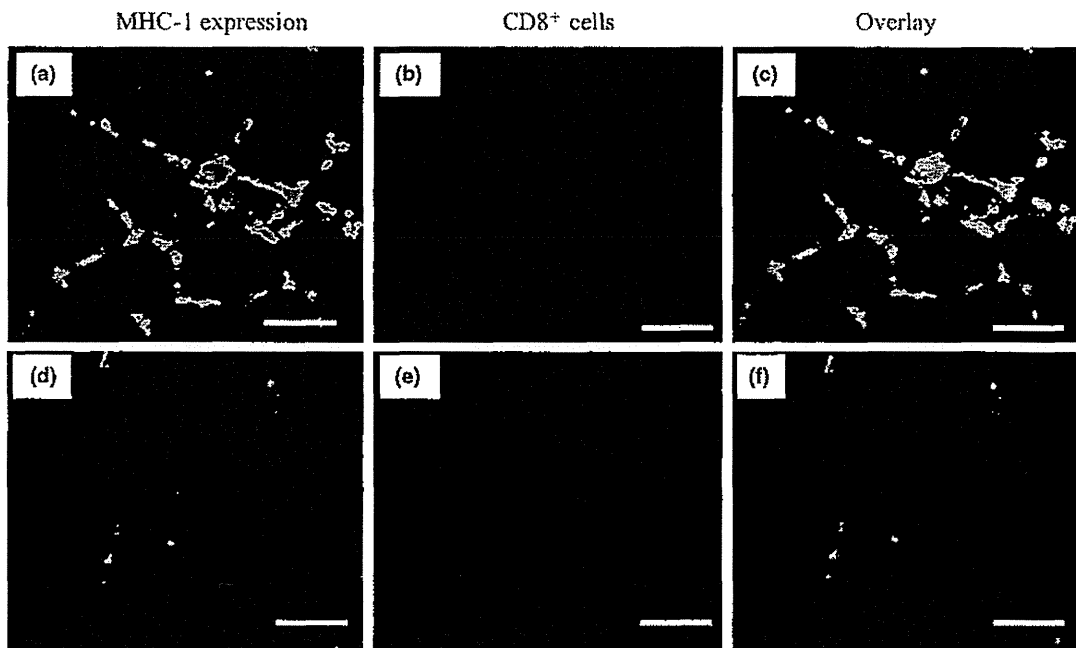


**Figure 3** Detection of the CD8/MHC-1 complex by double staining for MHC-1 and CD8 antigens by immunofluorescence. (a) Histologically healthy non-necrotic fibers expressing histocompatibility complex (MHC)-1antigens (green color). (b) CD8<sup>+</sup> cells surrounding and invading histologically healthy non-necrotic muscle fibers (red color). (c) Overlay of both histologically healthy non-necrotic fibers expressing MHC-1 antigens (green color) and CD8<sup>+</sup> cells invading them (red color). (d) Histologically healthy non-necrotic fibers not expressing MHC-1 antigens (no green color). (e) CD8<sup>+</sup> cells surrounding and invading the histologically healthy non-necrotic muscle fibers (red color). (f) Overlay of both histologically healthy non-necrotic fibers not expressing MHC-1 antigens (no green color) and CD8<sup>+</sup> cells invading them (red color). Bars, 100  $\mu$ m.

5–50 cells/ $\times$ 200 field (F); mean 31 (13.7)/F compared with HTLV-1-negative PM patients [range 3–27 cells/F; mean 11 (8.6)/F;  $P = 0.0008$ ; Fig. 2a,b,e]. There was no significant difference between the number of perimysial inflammatory cells in the HTLV-1-positive PM [range 0–27 cells/F; mean 9 (8.2)/F] and HTLV-1-negative PM groups [range 5–25/F; mean 11 (6.4)/F; Fig. 2c–e]. Regarding the subsets of inflammatory infiltrates, CD8<sup>+</sup> and CD4<sup>+</sup> cells were predominant in the endomysium and perimysium in both groups, respectively (Fig. 2f,g). The subsets of infiltrating CD4<sup>+</sup>, CD8<sup>+</sup>, CD68<sup>+</sup> and CD20<sup>+</sup> cells in the endomysium were 30%, 46%, 21% and 3%, in the HTLV-1-positive PM group, and 31%, 48%, 19% and 2% in the HTLV-1-negative PM group, respectively. The subsets of infiltrating CD4<sup>+</sup>, CD8<sup>+</sup>, CD68<sup>+</sup> and CD20<sup>+</sup> cells in the perimysium were 48%, 37%, 14% and 1% in the HTLV-1-positive PM group, and 44%, 37%, 16% and 3% in the HTLV-1-negative PM group, respectively. There were no apparent differences in the subsets of infiltrating cells between the two groups.

#### Necrotic fibers are less common in HTLV-1-positive patients

Necrotic fibers, which were counted and averaged out of 200 fibers, were less frequently observed in HTLV-1-positive patients [Fig. 4a; range 0–4/200 fibers; mean 2 (1.75)] than in HTLV-1-negative patients [Fig. 4b; range 1–25/200 fibers; mean 6 (7);  $P = 0.0201$ ; Fig. 4c].

#### Regenerative activity is more common in HTLV-1-positive PM

The number of fibers expressing regenerative activity was determined using anti-NCAM and anti-MHCn antibodies. NCAM-positive fibers tended to be more common in HTLV-1-positive PM [Fig. 5a; range 2–25/200 fibers; mean 10 (8.1)] than in HTLV-1-negative PM [Fig. 5b; range 0–20/200 fibers; mean 6 (5.8)];  $P = 0.063$ ; Fig. 5e). MHCn-positive staining fibers, which are a more specific regenerative marker, were significantly more common in HTLV-1-positive PM [Fig. 5c; range 3–25/200 fibers; mean 11

**Table 1** Detailed clinical and laboratory data of all 21 patients

Case serial number	Age/sex	Duration of illness (months)	Laboratory data										Response to CS treatment	Site of biopsy
			Tissue nested PCR	Serum anti HTLV-1 antibodies	Tissue viral preload (copy/10 <sup>4</sup> cells)	CK (IU/L)	Anti jo-1	ANA	Muscle weakness	Gait	EMG			
Po 1	50/F	120	+	+	1	400	-	-	Moderate S P > D	D	Myopathic	Effective	Biceps brachii	
Po 2	59/F	12	+	+	1627	1390	-	-	Mild S P > D	N	Myopathic	Effective	Biceps brachii	
Po 3	59/F	12	+	+	1	1100	-	-	Moderate S P > D	D	Myopathic	Effective	Biceps brachii	
Po 4	56/F	24	+	+	4	370	-	-	Moderate S P > D	M	Myopathic	Effective	Biceps brachii	
Po 5	63/F	24	+	+	316	1538	-	-	Mild S P > D	M	Myopathic	Effective	Biceps brachii	
Po 6	62/F	144	+	+	7	349	-	-	Mild S P > D	M	Myopathic	Effective	Biceps brachii	
Po 7	53/M	1	+	+	633	4742	-	-	Mild S P > D	N	Myopathic	Effective	Biceps brachii	
Po 8	66/M	48	+	+	7	2924	+	-	Mild S P > D	M	Myopathic	Effective	Biceps brachii	
Po 9	51/F	60	+	+	1	206	-	-	Moderate S P > D	D	Myopathic	Effective	Biceps brachii	
Po 10	70/M	240	+	+	2063	355	-	-	Mild S P > D	M	Myopathic	Effective	Quadriceps femoris	
Po 11	35/F	36	+	+	13	4000	-	-	Moderate S P > D	D	Myopathic	Effective	Biceps brachii	
Neg 1	53/F	24	-	-	NA	599	-	-	Moderate S P > D	D	Myopathic	Effective	Biceps brachii	
Neg 2	65/F	8	-	-	NA	2400	-	-	Moderate S P > D	D	Myopathic	Effective	Biceps brachii	
Neg 3	57/F	12	-	-	NA	4525	-	-	Mild S P > D	M	Myopathic	Effective	Biceps brachii	
Neg 4	60/F	12	-	-	NA	330	-	-	Moderate S P > D	D	Myopathic	Effective	Biceps brachii	
Neg 5	50/F	2	-	-	NA	840	-	-	Mild S P > D	N	Myopathic	Effective	Biceps brachii	
Neg 6	62/M	10	-	-	NA	523	-	-	Mild S P > D	M	Myopathic	Effective	Biceps brachii	
Neg 7	36/F	2	-	-	NA	7760	-	-	Mild S P > D	N	Myopathic	Effective	Biceps brachii	
Neg 8	67/F	6	-	-	NA	2895	-	-	Moderate S P > D	D	Myopathic	Effective	Biceps brachii	
Neg 9	58/F	1	-	-	NA	834	-	-	Mild S P > D	N	Myopathic	Effective	Biceps brachii	
Neg 10	56/M	4	-	-	NA	561	-	-	Mild S P > D	M	Myopathic	Effective	Biceps brachii	

Muscle strength score: 5, normal; 4, good; 3, fair; 2, poor; 1, trace; 0, no muscle contraction. +, positive; -, negative. ANA, anti-nuclear antibody; anti jo-1, antibody antihistidyl t-RNA synthetase antibody; CK, creatine kinase; CS, corticosteroid; D, distal muscle strength; D, disturbed gait; EMG, electromyography; HTLV-1, human T-lymphotropic virus type 1; N, normal gait; NA, not assessed; M, mildly changed gait; P, proximal muscle strength; PCR, polymerase chain reaction; S, symmetrical muscle strength.

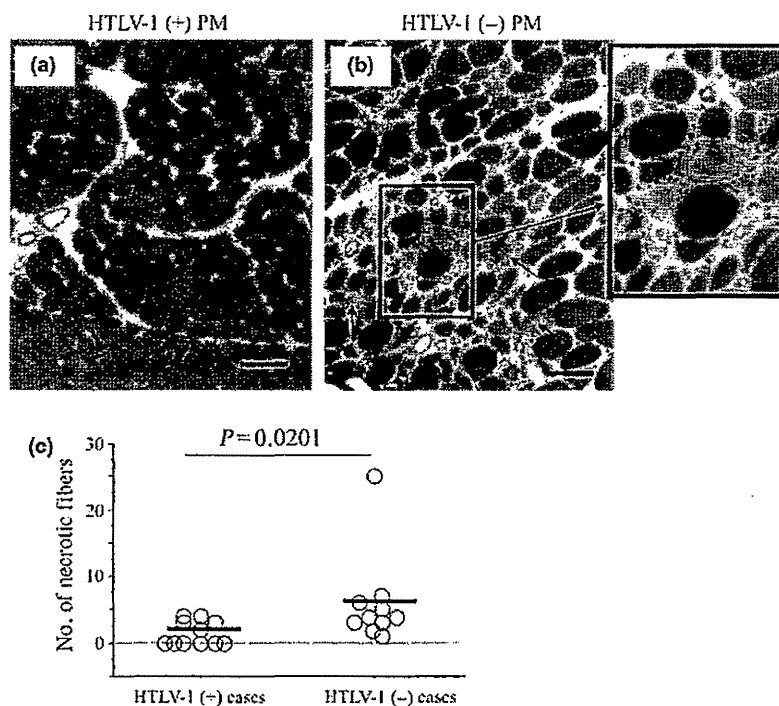


**Figure 4** Necrotic fibers in cross-sections of muscles biopsied from human T-lymphotropic virus type 1 (HTLV-1)-positive and HTLV-1-negative PM patients. (a) Very few necrotic fibers are seen in HTLV-1-positive polymyositis (PM); most fibers are histologically viable and healthy. (b) A greater number of necrotic fibers are seen in HTLV-1-negative PM (arrows); inset shows higher magnification of frequently seen necrotic fibers invaded by inflammatory phagocytic cells. (c) Combined data for all study patients. Significantly greater numbers of necrotic fibers are seen in HTLV-1-negative PM than in HTLV-1-positive PM ( $P = 0.0201$ ; Mann-Whitney  $U$ -test). Bars (a)–(b) 100  $\mu\text{m}$ .

(8.3)] than in HTLV-1-negative PM [Fig. 5d; range 0–20/200 fibers; mean 6 (5.5);  $P = 0.045$ ; Fig. 5e]. There was no apparent difference between the groups regarding the staining profiles for the other antibodies including anti-HSP47 (a marker for subsequent fibrotic processes), perforin (a cytolytic protein and a marker of apoptosis induced by  $\text{CD8}^+$  and natural killer cells) and thrombomodulin, which has anti-thrombotic, anti-inflammatory and anti-apoptotic activities.

#### CCO activity is decreased in HTLV-1-positive PM

Using normal controls as a reference (Fig. 6a), peripheral fields were not examined to avoid dryness artifacts in the samples. The examined central fields were separated from the edges of the sections by at least one field distance. Partially decreased CCO-stained (Fig. 6c) or completely CCO-negative fibers (Fig. 6d) were frequently found in 9 of 11 HTLV-1-positive PM patients, but only in 3 of 10 HTLV-1-negative PM patients (Fig. 6b). In all 21 PM patients, the number of fibers with partially decreased CCO activity or completely CCO-negative that were counted out of 200 fibers was higher in HTLV-1-positive PM patients [range 0–28/200 fibers; mean, 7 (8)] than in HTLV-1-negative PM patients [range 0–1/200 fibers; mean 1 (1);  $P = 0.0031$ ; Fig. 6e].

The staining profile of SDH enzyme histochemistry was normal in all HTLV-1-positive and HTLV-1-

negative PM cases except for one case from each group that showed mild reduction in 1–2 fibers/200 fibers.

#### Mitochondrial morphological abnormalities in HTLV-1-positive PM

We examined semi-thin sections from seven HTLV-1-positive patients showing partially reduced CCO-staining or completely CCO-negative fibers. Sections that had areas with inflammatory infiltrates and variable-sized closely backed myofibers without artifacts and separated by a thin endomysium were selected for ultrathin sections. Morphologically abnormal mitochondria were found on examination of these ultrathin sections (range 8–61%; mean 30%). To avoid misinterpretation of preparation or fixation artifacts, we only considered abnormal mitochondria in well-fixed fields with intact surrounding sarcoplasm filled with closely packed myofibrils arranged in a precise manner without any contraction artifacts; other adjacent mitochondria showed slight swelling, but showed intact unseparated inner and outer membranes, and intact homogenous matrices and cristae. The morphologically abnormal mitochondria showed high-amplitude abnormal swelling without membrane separation, irregular or bizarre shapes, membrane disruption, matrix fragmentation, loss of cristae (Fig. 7c,e), and myelin-like structures (Fig. 7d). In